Modelling interactions that determine core gut microbiome stability to predict microbiome perturbation by opportunistic pathogens

P.T. van Leeuwen[1], S. Brul[1], J. Seppen[2], M.T. Wortel[1]

[1] Molecular Biology and Microbial Food Safety, Swammerdam Institute for Life Sciences, University of Amsterdam, Amsterdam, The Netherlands
[2] Tytgat Institute for Liver and Intestinal Research, Amsterdam University Medical Centers, Location AMC, 1105 BK Amsterdam, The Netherlands

The gut microbiome plays a crucial role in host homeostasis, with implications for nutrition, immune development, metabolism, and protection against pathogens. Changes in microbiome composition are associated with host health and after microbial shifts, opportunistic pathogens have a unique chance to invade and overgrow the microbiome However, the complexity of the microbiome inhibits understanding of cause and consequence. This study describes a species interaction model to predict gut microbiome stability. This method aids in understanding perturbation of the gut microbiome by opportunistic pathogens *Escherichia coli* and *Bacteroides ovatus* and validate predictions in co-culture growth experiments. Despite their inherent differences in growth rates and interaction with gut commensals, both *E. coli* and *B. ovatus* can successfully invade an established consortium. However, the mechanisms of invasion differ; *B. ovatus* replaces an original consortium bacterium, whereas *E. coli* integrates into the established microbiome. This research enhances our understanding of microbial invasion processes and their implications for gut microbiome stability and host health.

Introduction

The intestine harbours a diverse community of microorganisms: the gut microbiome. The largest constituent of the gut microbiome are bacteria of four phyla: Firmicutes, Bacteroidetes, Proteobacteria, and Actinobacteria (Jandhyala *et al.* 2015). The microbiome is intricately involved in various facets of host homeostasis, including nutrition, immune development, metabolism, and protection against pathogens (O'Hara and Shanahan 2006). Microbiomes exhibiting stability, characterized by minimal alterations in composition following perturbations, are commonly associated with a state of homeostasis and overall well-being. In contrast, dysbiosis, marked by an unstable or disrupted microbiome, is often linked to a range of health issues, including inflammatory bowel disease and other gastrointestinal disorders (Ley *et al.* 2005, 2005; Ridaura *et al.* 2013; Carding *et al.* 2015; Chang and Lin 2016; Saffouri *et al.* 2019; Fassarella *et al.* 2021; Sultan *et al.* 2021; Santana *et al.* 2022).

To better research the causality of the relation between microbiome composition, competition and subsequent host effects, entire microbiomes would ideally be studied *in vitro*. The enormous complexity of the microbiome and the restrictions on the growth conditions for the different microbes inhibit replicability with this method. To address this issue, researchers have cultured the microbes derived from faeces of host subjects to retain complexity and analysing outcomes based on these faecal samples (Atarashi *et al.* 2013). The results of these studies are, however, often hard to replicate because of the different microbial compositions between subjects' faeces. The use of synthetic microbial communities (SynComs) can reduce the complexity, whilst keeping the functional profile of the gut microbiome. Moreover, factors such as community size and species interactions, that influence community stability, are being preserved in well-constructed Syncoms (Shetty *et al.* 2022;

van Leeuwen *et al.* 2023) and SynComs can be combined with computational studies to enhance the understanding of cause-and-effect relationships.

Escherichia coli and *Bacteroides ovatus,* two prevalent members of the human gut microbiota, are associated with disease. Both bacteria can be considered as commensals and opportunistic pathogens, possessing mechanisms to exploit host vulnerabilities and transition to pathogenic behavior under certain environmental conditions (Saitoh *et al.* 2002; Kaper, Nataro and Mobley 2004; Tenaillon *et al.* 2010) . *E. coli*, a gram-negative bacterium, comprises a diverse group of strains, with some capable of causing infections ranging from mild gastrointestinal disturbances to severe systemic illnesses such as urinary tract infections and sepsis (Kaper, Nataro and Mobley 2004; Tenaillon *et al.* 2010). *B. ovatus*, a predominant member of the Bacteroides genus, is implicated in various infections, particularly in immunocompromised individuals (Saitoh *et al.* 2002). The ability of these bacteria to invade and persist within the human system is multifaceted, involving factors such as adhesion to host epithelial cells, evasion of immune responses, and the production of virulence factors (Aubel, Darfeuille-Michaud and Joly 1991; El-Baky *et al.* 2020). Furthermore, their capacity to thrive in the gut amidst a complex microbial community raises questions about the mechanisms by which they outcompete or coexist with other bacterial species (Winter *et al.* 2013; Fultz *et al.* 2021).

For *in-silico* analysis of microbiomes, researchers use diverse modelling frameworks, categorized into species interactions and consumer-resource models (Faust and Raes 2012; van den Berg *et al.* 2022). A well-known species interactions model is the generalized Lotka-Volterra model (gLV). Generalized Lotka-Volterra equations, an ordinary differential equation model, uses a concise set of parameters deducible from time-series data and can be used to simulate the dynamics of interacting species in ecological systems, considering factors like competition and predation. For example, Venturelli *et al.* (2018) used gLV models to predict community dynamics and de Vos *et al.* (2017) used a modified gLV model to predict compositional dynamics in communities composed of microorganisms associated with urinary tract infections. These models come with inherent limitations, such as its incompatibility with batch cultures due to limited growth data and it required considering direct interactions between species, as highlighted by Picot (2023), Ye (2014) and Rapaport (2020). Consumer-resource models circumvent some of the drawbacks of Lotka-Volterra models. Consumer-resource models are ecological models that depict communities of consumer species competing for a shared pool of resources. Unlike direct species interactions, all interactions in consumer-resource models are mediated through resource dynamics (D'hoe *et al.* 2018). However, they demand extensive data covering the consumption rates of each interaction partner for accurate depiction, representing a crucial consideration in their application within microbial community studies. Even with extensive data inputs, these models sometimes struggle to perform well , especially during evolution, underscoring the deeper intricacies inherent in modelling ecological processes (Hiltunen *et al.* 2014).

Our objective is to study interactions between gut microbiota and how these affect the stability of a SynCom and its invasion by opportunistic pathogens. In this work, we first describe the selection of a representative human gut SynCom. Then we investigate pairwise interactions by studying growth with supplemented supernatants of other bacteria. Next, we use a gLV model to study the importance of these interactions in co-cultures up to four species. Finally, we make predictions about the invasion dynamics of *E. coli* and *B. ovatus*.

Table 1: Bacterial species used in this study. We generalized the metabolism of the bacteria in three categories: Principal, Intermediate and Endpoint. Principal covers bacteria that metabolize large complex carbon structures like dietary fiber . Intermediate covers bacteria that metabolize carbohydrates into, for example, acetate. Endpoint denotes bacteria which metabolize the acetate into butyrate. The health status: +, - and +/- indicates that the published data on this bacterium has been associated with health, metabolic disease and mixes reports respectively.

Metabolism	Species	Phylum	Health status	Legend colour	Abbreviation
Principal	*Akkermansia muciniphila*	Verrucomicrobia	+		AM
	Bifidobacterium adolescentis	Actinobacteria	+		BA
	Bacteroides thetaiotaomicron	Bacteroidetes	+		BT
	Bacteroides ovatus	Bacteroidetes	-		BOV
Intermediate	*Escherichia coli*	Proteobacteria	-		EC
	Lactobacillus johnsonii	Firmicutes	+		LJ
	Blautia obeum	Firmicutes	+		BOB
	Lachnospiraceae bacterium	Firmicutes	+/-		LB
Endpoint	*Roseburia intestinalis*	Firmicutes	+		RI
	Faecalibacterium prausnitzii	Firmicutes	+/-		FP

Results

Selection of the Human Gut SynCom

We construct SynComs from bacterial strains that are known to be present in the western human gut and have been characterized in terms of their association with health or disease (Table 1) (Rinninella *et al.* 2019; Pittayanon *et al.* 2020; Haneishi *et al.* 2023). Specifically, we selected strains that have been previously identified as being associated with beneficial effects on human health and strains that have been identified as being associated with disease. Furthermore, we made sure all strains we wanted to use were obtainable (Figure 1). Additionally, to increase the likelihood of co-growth in a laboratory setting we selected species that were previously used in SynComs (Petrof *et al.* 2013; Desai *et al.* 2016; Mark Welch *et al.* 2017; D'hoe *et al.* 2018; Venturelli *et al.* 2018; Ziesack *et al.* 2018; El Hage 2019; Gutiérrez and Garrido 2019). In summary, the species selected all have clearly defined functions within the microbiome, have known sequences of at least their 16S region, and are all culturable under similar anaerobic conditions in a lab environment. Then we selected a set of ten species that were representative of gut composition on a phylum level, making sure all large categories of functions were covered (Arumugam *et al.* 2011; Costea *et al.* 2018; van Leeuwen *et al.* 2023). Ten bacteria were then left that can be used as an incidental backup. The metabolic functions were identified for all bacteria and categorized as principal, intermediate or endpoint metabolizers (Table 1) (Petrof *et al.* 2013; Desai *et al.* 2016; Mark Welch *et al.* 2017; D'hoe *et al.* 2018; Venturelli *et al.* 2018; Ziesack *et al.* 2018; El Hage 2019; Gutiérrez and Garrido 2019). The principal metabolizers are bacteria that have the capability of metabolizing starches into simpler sugars. The intermediate metabolizers can take those simpler sugars and metabolize these into among others acetate. The endpoint metabolizers can produce butyrate from the sugars and acetate. Communities with members of all three groups are likely more stable because of the possibility of cross feeding.

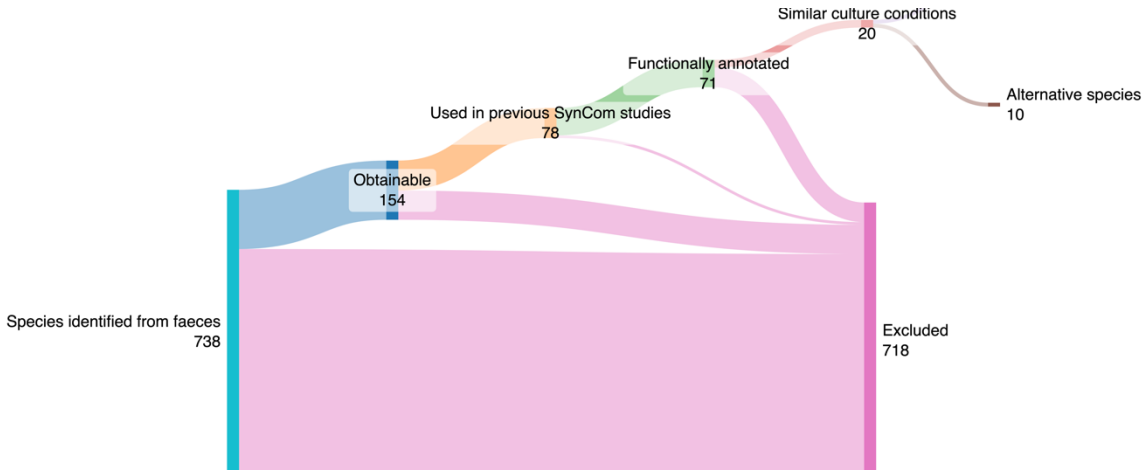

Figure 1: The inclusion of bacterial strains. Starting with 738 bacteria, we used different filtering steps to reduce the number of strains to be used in our experimental setup down to 10. The 10 alternative species are bacteria that can fulfil similar functions from the included bacteria and were thus considered as back-up resources.

Pairwise interactions are not explained by metabolic type or phylogeny

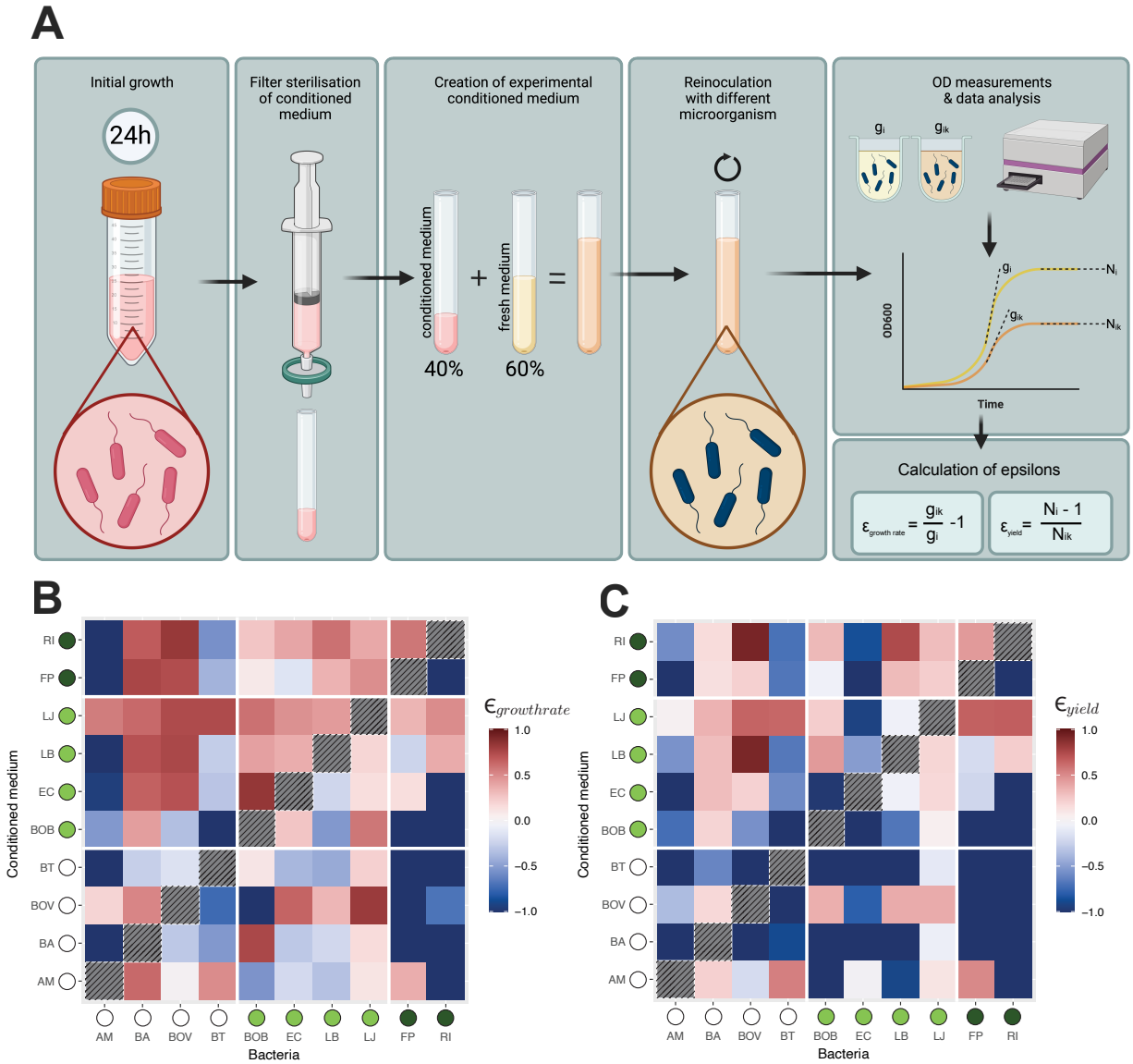

Figure 2: Pairwise interactions deduced from conditioned media growth. A graphical abstract of how the experiment was conducted using conditioned medium. **B** The epsilon growth rate is defined as the log of the growth rate in conditioned medium divided by the growth rate in monoculture. **C** The epsilon yield is defined similarly. The circles indicate the category of metabolism, being principal (white), intermediate (light green) and endpoint (dark green).

To investigate the interactions of bacteria in a pairwise manner, we analysed the main growth parameters (growth rate, yield, and lag phase), for each bacterium grown in the supernatant of all the other bacteria (Figure 2). In terms of growth rate, a clear trend was observed that endpoint metabolizers higher growthrate in the spent medium of other bacteria compared to the control (top two rows of Figure 2A). Notably, *Roseburia intestinalis, Bacteroides ovatus, Lactobacillus jhonsonii,* and *Lachnospiracea bacterium* create favourable environments, fostering the growth of other species (Supplementary Figure S1). No discernible pattern in yield was observed as a direct consequence of the metabolic functions of the bacteria (Figure 2C). We identified a significant proportion (31.1%) of the interactions to be null interactions, which we defined as the effect size being smaller than 25% compared to the controls (Supplementary figure 2). 45.6% of the interactions were of negative nature and 23.3% positive.

Pairwise interactions improve predictions of co-cultures up to four species

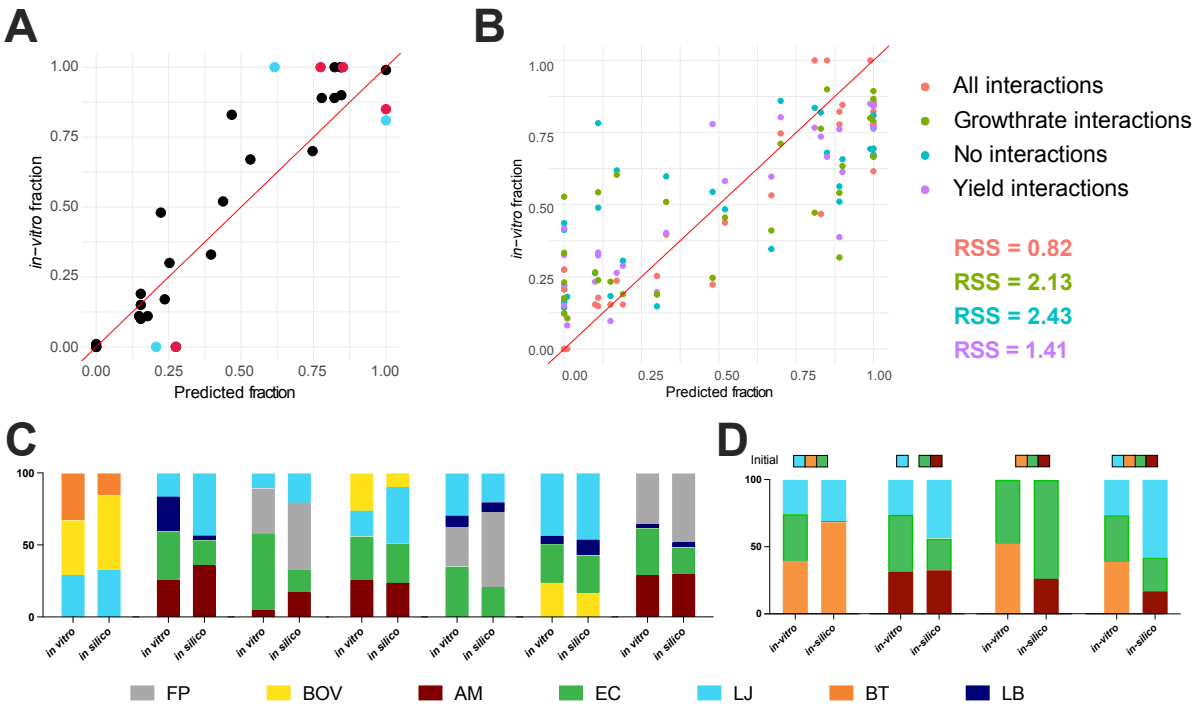

Figure 3: **Validation of the model predictions with co-cultures of two to four bacteria. A** The proportions of all two-species combinations plotted against *in vitro* biculture data analysed using a linear regression. The black line shows the linear regression (R^2 = 0.78), the dotted line indicates the diagonal. The red and blue data points indicate bicultures with either *Bifidobacterium adolescentis* or *Lactobacillus jhonsonii*. **B** The model was also plotted using less parameters. **C** proportions of endpoint yield of the bacteria plotted against the *in silico* predicted proportions of tri- and quad cultures. **D** shows the communities with predicted dropout strains, with their initial inoculation given in the squares right of the bars.

To predict stable communities used later for the invasions, we used an adapted gLV model to model interactions involving both growth rate and yield (de Vos *et al.* 2017)(Equation 2). We changed the model such that it also contains a total biomass limitation to ensure there are no runaway combinations. The model is parameterized on our quantitative interaction data. This model describes the population dynamics within polymicrobial communities, enabling quantitative predictions regarding the stability and dynamics of diverse isolate Syncoms.

To assess the accuracy of the model, the model predictions were compared against growth data obtained through co-cultures with relative abundances quantified by qPCR (Figure 3). The predicted proportions of bacteria in bicultures exhibited a strong correlation with the experimentally measured proportions (R^2 = 0.78, $p < 0.01$). Combinations involving *Bifidobacterium adolescentis* and *L. jhonsonii* overgrew their co-habiting species on 14 out of the 18 occasions, which was not predicted by the model (Figure 3A, red and blue points).

To test whether the interactions contribute to a better prediction, thereby testing whether the predictions measured in supernatant are representative for the interactions in co-cultures, we conducted an analysis where specific parameters were systematically removed to evaluate their impact on correlation (see Figure 3C). We observed that the omission of interactions led to a decreased model fit, with the yield interaction parameter demonstrating the most significant improvement in goodness of fit (Supplementary figure 3).

The model performance was subsequently evaluated by conducting validation experiments using consortia of three and four species that were predicted to be stable, i.e. at least 2 times the starting population size after 24 hours per microorganism. The *in vitro* replicates never differed more than 7.4% from each other. Out of the possible 17 communities, six were randomly selected and validated to be stable *in vitro*; although the relative abundances sometimes deviate (Figure 3B), all microorganisms that were predicted to be there could be detected.

Next, we aimed to evaluate the model's ability to predict drop-out strains in unstable bacterial communities (Figure 3C). Here, we defined an unstable community as one where a strain is eliminated from the community within the first 24 hours of growth. In three- and four-species communities, the model achieved an accurate prediction of communities with dropouts in 75% of the cases. The model had difficulty to accurately predict the specific species that would drop out from the community.

E. coli and *B. ovatus* invade in half of the communities but differ in mode of entry

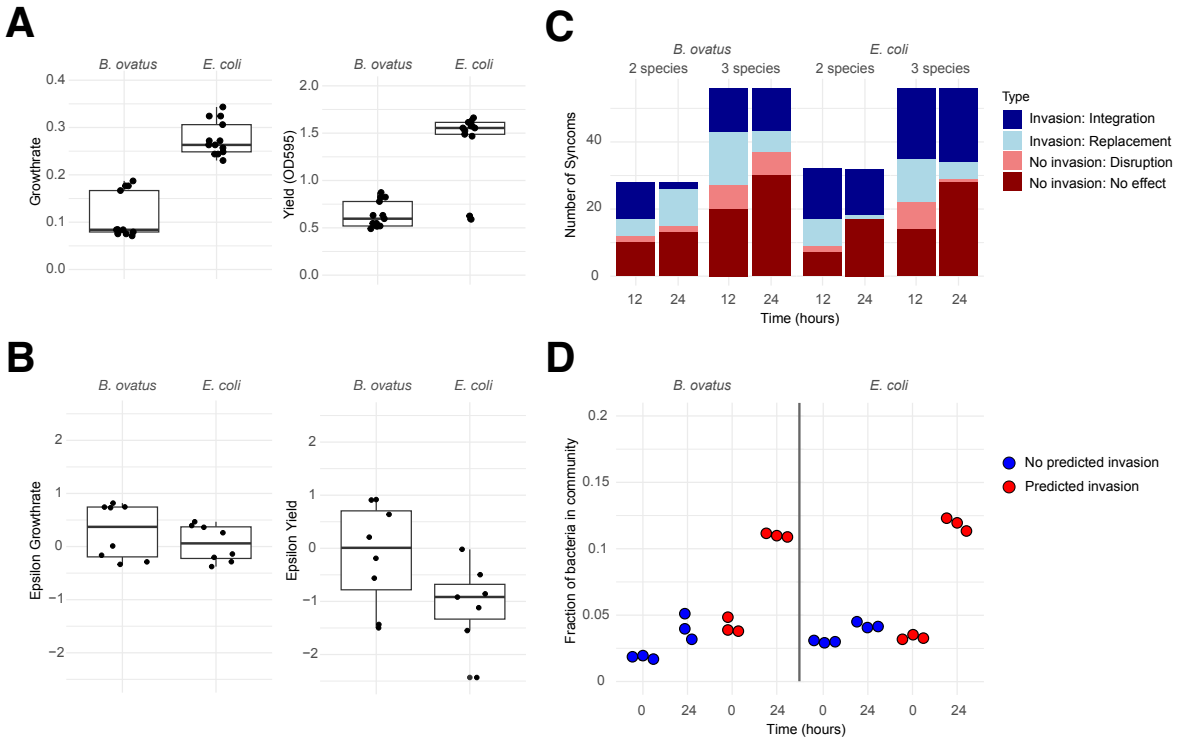

Figure 4: **Invasion dynamics of *E. coli* and *B. ovatus* in two- and three species established Syncoms**. **A** The measured growth parameters of *E. coli* and *B. ovatus*. Each point in the boxplot shows a separate culture. **B** The calculated $\varepsilon_{growthrate}$ and ε_{yield} showing the effect of other species on *E. coli* and *B. ovatus*. **C** Invasion dynamics of these species were predicted in established Syncoms at 12 and 24 hours post-initial growth, categorized into four outcomes: integration (dark blue), replacement (light blue), disruption (light red), and no effect (dark red). Integration indicates successful invasion and integration into the established Syncom, while replacement signifies the replacement of an initial species by the invader. Disruption occurs when the invading species destabilizes the Syncom despite minimal presence, and no effect denotes no invasion and no discernible impact. **D** *In vitro* cell growth analysis was conducted on both 2 and 3 species established Syncoms devoid of initial *E. coli* or *B. ovatus*. The Syncoms for which invasion was predicted to be successful are depicted in red, blue depicts non-successful predicted invasion.

E. coli and *B. ovatus* have different growth characteristics: *E. coli* has a high growth rate and yield when cultivated in isolation, and predominantly negative interactions with other bacteria (Figure 4A and B). In contrast, *B. ovatus has* a significantly lower growth rate and yield than *E. coli*, but more positive interactions. We wondered if the bacteria, with their inherent differences, also exhibit other behaviour when they are invading in an already established community. We used our model to *in silico* predict the dynamics after invasion and predict that *B. ovatus* more often replaces one of the resident species,

while *E. coli* integrates with the resident species (Figure 4C). The establishment of the initial consortium significantly decreases the success rate of invading species, the earlier the invasion, the more likely that the invasion is successful (Supplementary Figure S5).

Some Syncoms exhibit resistance to invasion when the invading microorganism is introduced together with the consortium, suggesting inherent barriers to invasion in certain ecosystems. Notably, a recurring pattern emerges in species that resist invasion by *E. coli* and *B. ovatus*. For *E. coli*, key antagonistic species include *B. adolescentis*, *B. thetaiotamicron*, and *B. obeum*, whereas for *B. ovatus*, significant antagonists include *B. obeum* and *F. prausnitzii* (Supplementary Figure S6). While these species were often, but not always, negatively influencing the invading species in the interaction experiments (Fig 2), they were not clear outliers and therefore, this antagonism cannot be predicted from direct interactions only. In contrast, *A. muciniphilia* frequently present in consortia where either *E. coli* and *B. ovatus* can successfully invade (Supplementary Figure S6).

To validate the model's predictions, we conducted invasion experiments with *E. coli* and *B. ovatus* in different consortia (Figure 4D). In consortia in which the invading species was predicted to invade, we observed a significant increase of the invading species, while the consortia that were predicted to withstand invasion, we did not observe an increase.

Discussion

We demonstrated that two opportunistic pathogens in the human gut microbiome have different growth characteristics and community interactions, and that the result of their invasion in established communities are different. We have shown that interactions measured in supernatant assays can be used to predict results of co-culture assays, showing that at least an important fraction of the interactions is mediated through the medium, even though we could not directly explain the sign of the interactions from the metabolic profile of each of the species (in agreement with (Shetty *et al.* 2022)).

E. coli, stands out as the best-characterized member of our consortia, and is a model for an opportunistic pathogen (Ruiz and Silhavy 2022). We show that *E. coli* is characterized by a high intrinsic growth rate and yield, but mostly experiences negative interactions with other species. A different opportunistic pathogen, *B. ovatus*, is characterised by low growth rates and positive interactions.

Contrary to previous research (de Vos *et al.* 2017; Venturelli *et al.* 2018; Dedrick *et al.* 2023), we found a significant proportion of positive interactions. We found a relatively large proportion of positive- and null interactions (~23% and ~32% respectively), compared to 10-15% positive interactions found previously. This is interesting in the light of recent papers stating negative (Palmer and Foster 2022) or positive (Kehe *et al.* 2021; Giri *et al.* 2022) interactions dominate in nature. For the gut microbiome, Venturelli *et al.* (2018) show that in their selection of microorganisms most interactions were negative, but the strongest interactions were positive, something we did not observe even while there is some overlap in species between these studies. The large prevalence of negative interactions in their study might originate from interference competition through bacteriocins and Type 6 Secretion Systems in addition to resource competition. Genomic analysis suggests that the gut is primarily dominated by interference competition (Ding *et al.* 2021; García-Bayona, Coyne and Comstock 2021). The ecological stress-gradient hypothesis suggests that positive interactions are more prevalent in harsher environments (Piccardi, Vessman and Mitri 2019; Martino, Picot and Mitri 2024). For gut species, Shetty *et al.* (2022) indicates that although bacterial species used were in competition for similar substrates, they were able to live in co-existence during growth on a mixture of dietary fibers. In the light of the stress-gradient hypothesis our results are quite surprising, as we are using a rich medium,

void of dietary fibers, in which each thrives on its own, which should according to this theory promote negative interactions. However, we find more negative than positive interactions, revealing that the prevalence of competitive and exploitative interaction dynamics appears to outweigh cooperation in the communities used in this research.

The gLV model is a model that takes only direct interactions into account and therefore has known limitations, particularly in nutrient-rich environments where it struggles to accurately predict interactions (Kettle *et al.* 2015; Dedrick *et al.* 2023). Despite our use of rich medium, the model performed well in predicting bacterial community dynamics, possibly due to our species being more adjusted to high nutrient conditions than the nasal cavity bacteria from Dedrick et al. (2023). We observed that *L. jhonsonii* and *B. adolescentis* were predicted to grow in symbiosis, often overgrew their partners, indicating that some interactions were missed by the model. This aligns with findings by Allison and Martiny (2008), Comte et al. (2013), and Beier et al. (2015), who noted the limitations of gLV in capturing complex microbial dynamics. It could be an interesting extension to fit a consumer resource model to improve these predictions, but previous work shows it can be difficult to fit them well to SynComs (Pinto *et al.* 2017; D'hoe *et al.* 2018) simpler gLV models have been successful in various contexts (de Vos *et al.* 2017; Venturelli *et al.* 2018; Shetty *et al.* 2022; Dedrick *et al.* 2023).

The selected bacteria in our research and those reported in previous studies overlap to a significant degree. This is to be expected, as we chose bacteria based on their functional profile, and prevalence in the human western gut (Rinninella *et al.* 2019). Notably, five specific bacteria emerged as common denominators between these studies and ours, being *F. prausnitzii, R. intestinalis, E. coli, B. ovatus* and *B. thetaoitamicron*. In our experiments, especially *F. prausnitzii* and *R. intestinalis* show to grow well in the spent medium of other bacteria, which can explain their prevalence in the human gut where bacterial interactions are inevitable. Both *F. prausnitzii* and *R. intestinalis* are able metabolize butyrate (Duncan 2002; Rios-Covian *et al.* 2015), *E. coli, B. ovatus* and *B. thetaoitamicron* can assist these fermenters by means of cross feeding, possibly explaining their prevalence and effects on other bacteria in our setup (Chia *et al.* 2020; Lindstad *et al.* 2021; Mary and Kapoor 2022). It would be interesting to test how our results change when SynComs are used that more resemble the gut microbiome of different geographical and cultural populations.

In our investigation into the stability of gut microbial communities and the invasion of opportunistic pathogens, we defined stability as the absence of dropout strains and the growth into polymicrobial communities. The system that we used is a simplification to *in vivo* situations, where stability is often defined by a return to initial densities following perturbation. Hence, perturbing stable systems that also contain one of the opportunistic pathogens of choice would be a logical next step. Furthermore, we think that it could be interesting to destabilizing stable communities, which could offer new therapeutic avenues. Despite focusing on a subset of ten bacteria, a fraction of the species present in the human gut, we observed a decrease in stable communities as community size increased. Future directions could involve expanding the species used in experiments, as demonstrated by De Vos et al. (2017), who found larger and more complex communities with a larger subset of 72 isolates. In our work, we focussed the invasion analyses on two bacterial opportunistic pathogens. Expanding this to other opportunistic pathogens could reveal whether all opportunistic pathogens fall into one of our suggested categories, or if there are various growth and interaction characteristics that could lead to opportunistic pathogens. We demonstrated that *B. ovatus* and *E. coli* have distinct growth characteristics and community interactions, which can be predicted through supernatant assays, although the metabolic profiles of each species do not directly explain these interactions.

Material and methods

Bacteria and growth conditions

Bacterial strains were obtained from the DSMZ culture collection, and their identity was confirmed through 16S rRNA sequencing using universal primers, 16S forward (5'-AGAGTTTGATCCTGGCTCAG-3'); reverse (5'-ACGGCTACCTTGTTACGACTT-3'). In this study, the following bacterial strains were used: *Akkermansia muciniphila* (DSM 22959), *Bacteroides ovatus* (DSM 1896), *Bacteroides thetaiotaomicron* (DSM 2079), *Bifidobacterium adolescentis* (DSM 20083), *Blautia obeum* (DSM 25238), Escherichia coli (DSM 18039), *Faecalibacterium prausnitzii* (DSM 107838), *Lachnospiraceae bacterium* (DSM 24404), *Lactobacillus johnsonii* (DSM 10533), and *Roseburia intestinalis* (DSM 14610). The strains were then grown in YCFA media anaerobic conditions using an anaerobic chamber filled with anoxic gas (10% H_2, 80% N_2, 10% CO_2) set at 37 degrees Celsius unless mentioned otherwise.

Conditioned medium preparation

We prepared conditioned medium according to De Vos *et al.* (2017). We first inoculated the bacteria in YCFA medium and grew them for 24 hours. After 24 hours, we measured the optical density (OD) of the culture to ensure that the bacteria had surpassed log phase growth (OD > 1). We then filtered out the bacteria using a 0.2-micron filter to obtain the conditioned medium. To increase the likelihood vital metabolites including minerals and vitamins were still present in sufficient amounts for subsequent growth of other bacteria, we mixed 60% fresh medium with 40% of conditioned medium.

Growth of bacteria in conditioned medium

For the growth experiments, bacteria were pre-cultured for 16 hours or until they reached logarithmic phase. The bacteria were then diluted to an OD of 0.05 in a mixture of fresh and conditioned medium as described above. All 10 bacteria were cultured in all 10 conditioned media mixes, resulting in a total of 100 combinations. The growth of the bacteria was monitored using a Byonoy plate reader at a wavelength of 595 nm for 24 hours in an anaerobic workstation (Whitley A35 Workstation, Don Whitley Scientific) under anaerobic conditions (10% H_2, 10% CO_2, 80% N_2) at 37 degrees Celsius.

SynCom growth

To grow the SynComs, the bacteria were first individually pre-cultured for 16 hours or until they reached logarithmic phase. Using OD-CFU correlations, the bacteria were diluted to a final combined OD of 0.05 to ensure that the same number of CFUs were used for the bacterial combinations. All SynCom cultures were grown for 24 hours in 8mL flasks. After 24 hours, the OD was measured. The SynCom cultures were then prepared for downstream applications, depending on the experimental setup.

SynCom Invasion assay

Initial consortia were cultivated for 24 hours starting at an OD600 of 0.05. Simultaneously, a preculture of the invading species was grown under identical conditions. After 24 hours, the OD600 of the initial consortia cultures was measured. The bacterial cultures were centrifuged at 13000 x g for 5 minutes, and the supernatant was discarded. The cell pellets were resuspended in fresh growth medium. The invading species was washed twice with PBS, and its OD600 was measured. The washed invading species was then introduced into the resuspended initial consortia at a final OD600 of 0.1. Followed by an additional 24-hour incubation period. Total DNA was isolated from the cultures and then used in a QPCR assay.

DNA isolation

DNA isolation was performed using a modified Phenol-Chloroform method. SynComs were grown for 24 hours as described above, and then centrifuged at max speed to pellet the cells. The pellet was resuspended in elusion buffer (10 mM Tris-HCl, pH 8.5). The suspension was then mixed with an equal volume of phenol:chloroform:isoamyl alcohol (25:24:1) to separate the DNA from other cell components. The mixture was centrifuged, and the DNA-containing aqueous layer was transferred to a new container. The DNA was subsequently precipitated by adding ethanol and ammonium acetate to a final concentration of 0.75M. The DNA was collected by centrifugation, washed with 70% ethanol, and dissolved in elution buffer. The purified DNA was then quantified using spectrophotometry and stored at -20 degrees Celsius for downstream applications.

qPCR workflow

To quantify the composition of each community, qPCR was used. Primers targeting the bacterial species of interest were designed using primer3plus (https://www.bioinformatics.nl/cgi-bin/primer3plus/primer3plus.cgi). The primers were designed to amplify either a specific region of the bacterial 16S rRNA gene or a specific gene for the focal species. The forward and reverse primers were designed to yield a PCR product of approximately 200 base pairs with a delta of 50 base pairs. The designed primers were tested against all the other bacterial species used in this study to verify their specificity and exclude any potential false positives. PCR amplification was performed using the primers and DNA templates from each species. The resulting amplicons were analysed by gel electrophoresis to confirm the expected product size and absence of nonspecific amplification. The SYBR green method was employed for quantitative PCR (qPCR) analysis. The qPCR reactions were performed in a total volume of 25 µL, containing 12.5 µL of SYBR green master mix, 1 µL of each forward and reverse primer (10 µM), 2 µL of template DNA, and 8.5 µL of nuclease-free water. Negative controls (no template DNA) were included in each run to monitor potential contamination. qPCR amplification was carried out using the Applied Biosystems 7300 Real-Time PCR with the following thermal cycling conditions: an initial denaturation step at 95°C for 5 minutes, followed by 40 cycles of denaturation at 95°C for 30 seconds, annealing at 60°C for 30 seconds, and extension at 72°C for 30 seconds. The fluorescence signal was measured at the end of each extension step.

Further data analysis of qPCR data

The quantification cycle (Cq) values were recorded for each sample. Standard curves were generated using known concentrations of bacterial DNA containing the target sequence. The Cq values of the samples were compared to the standard curve to determine the initial bacterial load in each sample. The data were analysed using rStudio to evaluate the presence and abundance of the bacterial species within the community. To ensure the accuracy and reliability of the qPCR results, all experiments were performed in triplicate, and the average Cq values were calculated. Additionally, positive controls containing known concentrations of the target bacterial species were included to assess the efficiency and sensitivity of the qPCR assay.

Modelling and data analysis

All data analysis was done in rStudio and Spyder IDE (version 5.4.3) using R version 4.3.1 and Python version 3.11.4 respectively (Van Rossum and Drake 2009; R Core Team 2022). The Sankey diagram was made using Sankeymatic (Bogart 2024). Growth parameters were extracted through the growth rates package (Petzoldt 2022). In R, the ε_{yield} and $\varepsilon_{growth\ rate}$ were calculated as shown in equation 1.

$$\varepsilon_{growth\ \ parameter} = \log\left(\frac{growth\ parameter\ conditioned\ medium}{growth\ parameter\ control}\right)$$

Equation 1: **The ε calculation for the growth rate and yield parameter.**

The growth parameters were used as input data for equation 2, adapted from de Vos by adding a term to limit the total biomass to twice their summed individual biomasses.

$$\frac{dN_i}{dt} = N_i g_i \max\left(0, 1 + \sum_{k \neq i} a_{ik} N_k\right)\left(1 - \frac{N_i}{\max\left(10^{-9}, 1 + \sum_{k \neq i} b_{ik} N_k\right)}\right)\left(1 - \frac{\sum_{k \neq i} N_k}{2n}\right)$$

Equation 2: **The adjusted ecological logistic growth model as used in this study.** The adjusted ecological logistic growth model has two main components, a growth rate component in which the maximum growth rate ($g_i$max) is used, as well as the growth rate of the focal species in the conditioned medium of all other species (a_{ik}) as seen in Figure 6. The second main component is the yield component, featuring the yield component which is the yield of a focal species in the conditioned medium of all other species (b_{ik}).

Our model has been parameterized using our own measurements: the maximum growth rates ($g_i \max$), the α values representing the growth interaction coefficients between different microbial species calculated as seen in equation 3.

$$\alpha_{ik} = \frac{g_{ik}}{gi} - 1$$

Equation 3: **The calculation for the α parameter.** g_{ik} in this equation is the growth rate of the focal species i in the conditioned medium of species k. g_i states for the growth rate of the species in control medium.

The β values representing the yield interaction coefficients between different microbial species calculated as seen in equation 4.

$$\beta_{ik} = \frac{N_i - 1}{N_{ik}}$$

Equation 4: **The calculation for the β parameter.** N_{ik} in this equation is the yield of the focal species i in the conditioned medium of species k. N_i states for the yield of the species in control medium.

The species are normalized by their monoculture maximal population density. The expected proportions of bacteria in the model are then calculated by numerically solving the system of ODEs using the solve_ivp function from the SciPy library. The resulting concentrations at different time points provide insights into the dynamic behaviour of the synthetic microbial community under specified conditions, allowing for the identification of stable communities and their proportions in the long run.

References

Allison SD, Martiny JBH. Resistance, resilience, and redundancy in microbial communities. *Proc Natl Acad Sci* 2008;**105**:11512–9.

Arumugam M, Raes J, Pelletier E *et al.* Enterotypes of the human gut microbiome. *Nature* 2011;**473**:174–80.

Atarashi K, Tanoue T, Oshima K *et al.* Treg induction by a rationally selected mixture of Clostridia strains from the human microbiota. *Nature* 2013;**500**:232–6.

Aubel D, Darfeuille-Michaud A, Joly B. New adhesive factor (antigen 8786) on a human enterotoxigenic Escherichia coli O117:H4 strain isolated in Africa. *Infect Immun* 1991;**59**:1290–9.

Beier S, Rivers AR, Moran MA *et al.* Phenotypic plasticity in heterotrophic marine microbial communities in continuous cultures. *ISME J* 2015;**9**:1141–51.

van den Berg NI, Machado D, Santos S *et al.* Ecological modelling approaches for predicting emergent properties in microbial communities. *Nat Ecol Evol* 2022;**6**:855–65.

Bogart S. nowthis/sankeymatic. 2024.

Carding S, Verbeke K, Vipond DT *et al.* Dysbiosis of the gut microbiota in disease. *Microb Ecol Health Dis* 2015;**26**:10.3402/mehd.v26.26191.

Chang C, Lin H. Dysbiosis in gastrointestinal disorders. *Best Pract Res Clin Gastroenterol* 2016;**30**:3–15.

Chia LW, Mank M, Blijenberg B *et al.* Bacteroides thetaiotaomicron Fosters the Growth of Butyrate-Producing Anaerostipes caccae in the Presence of Lactose and Total Human Milk Carbohydrates. *Microorganisms* 2020;**8**:1513.

Comte J, Fauteux L, Giorgio PAD. Links between metabolic plasticity and functional redundancy in freshwater bacterioplankton communities. *Front Microbiol* 2013;**4**, DOI: 10.3389/fmicb.2013.00112.

Costea PI, Hildebrand F, Arumugam M *et al.* Enterotypes in the landscape of gut microbial community composition. *Nat Microbiol* 2018;**3**:8–16.

Dedrick S, Warrier V, Lemon KP *et al.* When does a Lotka-Volterra model represent microbial interactions? Insights from in vitro nasal bacterial communities. *mSystems* 2023;**0**:e00757-22.

Desai MS, Seekatz AM, Koropatkin NM *et al.* A Dietary Fiber-Deprived Gut Microbiota Degrades the Colonic Mucus Barrier and Enhances Pathogen Susceptibility. *Cell* 2016;**167**:1339-1353.e21.

D'hoe K, Vet S, Faust K *et al.* Integrated culturing, modeling and transcriptomics uncovers complex interactions and emergent behavior in a three-species synthetic gut community. Morgan X, Garrett WS (eds.). *eLife* 2018;**7**:e37090.

Ding M, Yang B, Ross RP *et al.* Crosstalk between sIgA-Coated Bacteria in Infant Gut and Early-Life Health. *Trends Microbiol* 2021;**29**:725–35.

Duncan SH. Roseburia intestinalis sp. nov., a novel saccharolytic, butyrate-producing bacterium from human faeces. *Int J Syst Evol Microbiol* 2002;**52**:1615–20.

El Hage R. Ability of a propionate-producing synthetic microbial consortium to restore functionality in a dysbiosed human gut microbiome. 2019.

El-Baky RAA, Ibrahim R, Mohamed D *et al.* Prevalence of Virulence Genes and Their Association with Antimicrobial Resistance Among Pathogenic E. coli Isolated from Egyptian Patients with Different Clinical Infections. *Infect Drug Resist* 2020;**13**:1221–36.

Fassarella M, Blaak EE, Penders J *et al.* Gut microbiome stability and resilience: elucidating the response to perturbations in order to modulate gut health. *Gut* 2021;**70**:595–605.

Faust K, Raes J. Microbial interactions: from networks to models. *Nat Rev Microbiol* 2012;**10**:538–50.

Fultz R, Ticer T, Ihekweazu FD *et al.* Unraveling the Metabolic Requirements of the Gut Commensal Bacteroides ovatus. *Front Microbiol* 2021;**12**, DOI: 10.3389/fmicb.2021.745469.

García-Bayona L, Coyne MJ, Comstock LE. Mobile Type VI secretion system loci of the gut Bacteroidales display extensive intra-ecosystem transfer, multi-species spread and geographical clustering. *PLOS Genet* 2021;**17**:e1009541.

Giri S, Yousif G, Shitut S *et al.* Prevalent emergence of reciprocity among cross-feeding bacteria. *ISME Commun* 2022;**2**:71.

Gutiérrez N, Garrido D. Species Deletions from Microbiome Consortia Reveal Key Metabolic Interactions between Gut Microbes. *mSystems* 2019;**4**:e00185-19.

Haneishi Y, Furuya Y, Hasegawa M *et al.* Inflammatory Bowel Diseases and Gut Microbiota. *Int J Mol Sci* 2023;**24**:3817.

Hiltunen T, Hairston N, Hooker G *et al.* A newly discovered role of evolution in previously published consumer-resource dynamics. *Ecol Lett* 2014;**17 8**:915–23.

Jandhyala SM, Talukdar R, Subramanyam C *et al.* Role of the normal gut microbiota. *World J Gastroenterol* 2015;**21**:8787–803.

Kaper J, Nataro J, Mobley H. Pathogenic Escherichia coli. *Nat Rev Microbiol* 2004;**2**:123–40.

Kehe J, Ortiz A, Kulesa A *et al.* Positive interactions are common among culturable bacteria. *Sci Adv* 2021;**7**:eabi7159.

Kettle H, Louis P, Holtrop G *et al.* Modelling the emergent dynamics and major metabolites of the human colonic microbiota. *Environ Microbiol* 2015;**17**:1615–30.

Ley RE, Bäckhed F, Turnbaugh P *et al.* Obesity alters gut microbial ecology. *Proc Natl Acad Sci U S A* 2005;**102**:11070–5.

Lindstad LJ, Lo G, Leivers S *et al.* Human Gut Faecalibacterium prausnitzii Deploys a Highly Efficient Conserved System To Cross-Feed on β-Mannan-Derived Oligosaccharides. *mBio* 2021;**12**:10.1128/mbio.03628-20.

Mark Welch JL, Hasegawa Y, McNulty NP *et al.* Spatial organization of a model 15-member human gut microbiota established in gnotobiotic mice. *Proc Natl Acad Sci* 2017;**114**:E9105–14.

Martino RD, Picot A, Mitri S. Oxidative stress changes interactions between 2 bacterial species from competitive to facilitative. *PLOS Biol* 2024;**22**:e3002482.

Mary PR, Kapoor M. Co-culture fermentations suggest cross-feeding among Bacteroides ovatus DSMZ 1896, Lactiplantibacillus plantarum WCFS1 and Bifidobacterium adolescentis DSMZ 20083 for utilizing dietary galactomannans. *Food Res Int* 2022;**162**:111942.

O'Hara AM, Shanahan F. The gut flora as a forgotten organ. *EMBO Rep* 2006;**7**:688–93.

Palmer JD, Foster KR. Bacterial species rarely work together. *Science* 2022;**376**:581–2.

Petrof EO, Gloor GB, Vanner SJ *et al.* Stool substitute transplant therapy for the eradication of Clostridium difficile infection: 'RePOOPulating' the gut. *Microbiome* 2013;**1**:3.

Petzoldt T. growthrates: Estimate Growth Rates from Experimental Data. 2022.

Piccardi P, Vessman B, Mitri S. Toxicity drives facilitation between 4 bacterial species. *Proc Natl Acad Sci U S A* 2019;**116**:15979–84.

Picot A, Shibasaki S, Meacock OJ *et al.* Microbial interactions in theory and practice: when are measurements compatible with models? *Curr Opin Microbiol* 2023;**75**:102354.

Pinto F, Medina DA, Pérez-Correa JR *et al.* Modeling Metabolic Interactions in a Consortium of the Infant Gut Microbiome. *Front Microbiol* 2017;**8**:2507.

Pittayanon R, Lau JT, Leontiadis GI *et al.* Differences in Gut Microbiota in Patients With vs Without Inflammatory Bowel Diseases: A Systematic Review. *Gastroenterology* 2020;**158**:930-946.e1.

R Core Team. *R: A Language and Environment for Statistical Computing*. Vienna, Austria: R Foundation for Statistical Computing, 2022.

Rapaport A, Nidelet T, Aida SE *et al.* About biomass overyielding of mixed cultures in batch processes. *Math Biosci* 2020:108322.

Ridaura VK, Faith JJ, Rey FE *et al.* Gut microbiota from twins discordant for obesity modulate metabolism in mice. *Science* 2013;**341**:1241214.

Rinninella E, Raoul P, Cintoni M *et al.* What is the Healthy Gut Microbiota Composition? A Changing Ecosystem across Age, Environment, Diet, and Diseases. *Microorganisms* 2019;**7**:14.

Rios-Covian D, Gueimonde M, Duncan SH *et al.* Enhanced butyrate formation by cross-feeding between Faecalibacterium prausnitzii and Bifidobacterium adolescentis. *FEMS Microbiol Lett* 2015;**362**:fnv176.

Romdhane S, Spor A, Aubert J *et al.* Unraveling negative biotic interactions determining soil microbial community assembly and functioning. *ISME J* 2022;**16**:296–306.

Ruiz N, Silhavy T. How Escherichia coli Became the Flagship Bacterium of Molecular Biology. *J Bacteriol* 2022;**204**, DOI: 10.1128/jb.00230-22.

Russel J, Røder HL, Madsen JS *et al.* Antagonism correlates with metabolic similarity in diverse bacteria. *Proc Natl Acad Sci* 2017;**114**:10684–8.

Saffouri GB, Shields-Cutler RR, Chen J *et al.* Small intestinal microbial dysbiosis underlies symptoms associated with functional gastrointestinal disorders. *Nat Commun* 2019;**10**:2012.

Saitoh S, Noda S, Aiba Y *et al.* Bacteroides ovatus as the Predominant Commensal Intestinal Microbe Causing a Systemic Antibody Response in Inflammatory Bowel Disease. *Clin Vaccine Immunol* 2002;**9**:54–9.

Santana PT, Rosas SLB, Ribeiro BE *et al.* Dysbiosis in Inflammatory Bowel Disease: Pathogenic Role and Potential Therapeutic Targets. *Int J Mol Sci* 2022;**23**:3464.

Shetty SA, Kuipers B, Atashgahi S *et al.* Inter-species Metabolic Interactions in an In-vitro Minimal Human Gut Microbiome of Core Bacteria. *Npj Biofilms Microbiomes* 2022;**8**:1–13.

Sultan S, El-Mowafy M, Elgaml A *et al.* Metabolic Influences of Gut Microbiota Dysbiosis on Inflammatory Bowel Disease. *Front Physiol* 2021;**12**.

Tenaillon O, Skurnik D, Picard B *et al.* The population genetics of commensal Escherichia coli. *Nat Rev Microbiol* 2010;**8**:207–17.

Van Rossum G, Drake FL. *Python 3 Reference Manual*. Scotts Valley, CA: CreateSpace, 2009.

van Leeuwen PT, Brul S, Zhang J *et al.* Synthetic microbial communities (SynComs) of the human gut: design, assembly, and applications. *FEMS Microbiol Rev* 2023;**47**:fuad012.

Venturelli OS, Carr AV, Fisher G *et al.* Deciphering microbial interactions in synthetic human gut microbiome communities. *Mol Syst Biol* 2018;**14**:e8157.

de Vos MGJ, Zagorski M, McNally A *et al.* Interaction networks, ecological stability, and collective antibiotic tolerance in polymicrobial infections. *Proc Natl Acad Sci* 2017;**114**:10666–71.

Winter S, Winter M, Xavier M *et al.* Host-Derived Nitrate Boosts Growth of E. coli in the Inflamed Gut. *Science* 2013;**339**:708–11.

Ye K, Wang H, Jiang Y *et al.* Development of interspecific competition models for the growth of Listeria monocytogenes and Lactobacillus on vacuum-packaged chilled pork by quantitative real-time PCR. *Food Res Int* 2014;**64**:626–33.

Ziesack M, Gibson T, Shumaker A *et al. Inducible Cooperation in a Synthetic Gut Bacterial Consortium Introduces Population Balance and Stability*., 2018.